

Energy balance of a drill-bit seismic source, part 1: Rotary energy and radiation properties

Flavio Poletto¹

ABSTRACT

An issue in seismic-while-drilling (SWD) technology is to characterize the dynamic and radiation properties of the drill-bit source working under different operational conditions. The energy requirements, power losses, local crack effects, radiation, and near-field effects associated with rotary drilling are analyzed to quantify the waves produced by an SWD vertical force acting in bounded and unbounded media. Results are expressed in terms of a complex integrated impedance and the equations for rotary drilling. The calculations — extended to the waves in the drill string — are used in part 2 of this paper (Poletto, 2005, this issue) to quantify the performance of actual drill-bit sources.

INTRODUCTION

The basic idea of the drill-bit seismic method is to use the drill bit as a source for while-drilling reverse vertical seismic profiling (VSP). The motivation and principles of the drill-bit seismic-while-drilling (SWD) technology have been described in several papers (e.g., Staron et al., 1988; Rector and Marion, 1991; Haldorsen et al., 1995; Miranda et al., 1996). Recently, interest has grown in the performance of the working drill-bit source to improve seismic-while-drilling VSP acquisition during poor drilling conditions (Poletto et al., 1997) and in using the drill-bit signal for downhole geosteering investigations (Lesso and Kashikar, 1996; Hokstad et al., 2001).

A main issue is the repeatability and controllability of the drill bit as a downhole acoustic source. In fact, drilling is performed with a large variety of configurations of mechanical drilling equipment, operational parameters, and geophysical settings that may change the properties of the radiated signal. For these reasons, the drill-bit method requires control of the acquisition conditions that characterize the effective applicability of SWD, as well as the properties of the radiated

signals. Methods based on signal-to-noise analysis (Haldorsen et al., 1995) and evaluation of statistical properties of the signal (Poletto et al., 2000) can help while-drilling quality control. However, it is common practice in SWD surveys to control and choose the acquisition parameters on the basis of experience, rather than on specific criteria, accounting for the dynamic conditions at which the drill-bit source is used. Hence, a more analytic approach is necessary to describe the behavior and to calculate the performance of the bit source. This new approach needs to be based on understanding the rotary-drilling process and the properties of the radiated fields.

Rotary drilling is the conventional technique used to excavate oil wells. This technology is extensively described in the drilling literature (e.g., Moore, 1986; Devereux, 1998). The process of breaking the rock is performed by the drill bit, which is mounted at the end of a drill string and lowered into the borehole (Figure 1a). The mechanical composition of the drill string as well as the SWD waves propagated in the drill string have been described, for instance, by Poletto et al. (2001). In the rotary action, by loading part of the drill-string weight, the bit is pushed against the rock, and is then rotated. Rotation can be provided by surface devices that rotate the drill string and/or by downhole motors or turbines hydraulically powered by the pressured mud flow in the pipes. Downhole motors can be used either with or without surface rotation (in rotary and sliding modes, respectively). The rotary energy imparted to the bit is expended in the rock-breaking action with the penetration rate monitored for drilling optimization. At the same time, part of this energy is radiated in the form of vibrations in the surrounding rock.

In part 1 of this paper, I consider the main energy requirements for drill-bit vibrations to be an effective seismic source. In part 2, I describe possible drilling conditions, together with the dynamic characteristics of bit sources and their frequency content. Calculations show that a drill-bit seismic source produces sufficient radiated energy while drilling intervals of a few meters and that the frequency bandwidth of the signal is broad, indicating that the drill bit can be used in SWD surface and downhole applications.

Manuscript received by the Editor December 17, 2001; revised manuscript received April 21, 2004; published online March 22, 2005.

¹Istituto Nazionale di Oceanografia e di Geofisica Sperimentale (OGS), Borgo Grotta Gigante 42/c, 34010 Sgonico, Trieste, Italy. E-mail: fpoletto@ogs.trieste.it.

© 2005 Society of Exploration Geophysicists. All rights reserved.

Part 1 of this paper is organized as follows. First, I introduce the basic equations of rotary-drilling energy. Second, I analyze the energy requirements and energy balance of the different processes involved in rock drilling. Third, I calculate the drill-bit radiation properties and the integrated-impedance conditions, assuming an axial source. Finally, I compare the results calculated by the drilling equations to the near-field vibrations and drill-string vibrations.

TOTAL DRILLING POWER

The performance of a drill-bit source is related to drilling-power conditions met during data acquisition. The total drilling power at the bit can be calculated by adding the torque power and the vertical work-per-unit time of the axial force (weight on bit, or WOB). We obtain the power (in kW):

$$W_{\text{drill}} = \frac{2\pi \text{rpm} \times \text{TOB}}{60} + \frac{\text{ROP} \times \text{WOB}}{3.6 \times 10^3}, \quad (1)$$

where rpm (rev/min), TOB (kNm), ROP (m/hour), and WOB (kN) denote rotary speed, torque on bit, rate of penetration, and weight on bit, respectively. Table 1 shows typical values of these drilling parameters. If we assume rpm = 120 rev/min, TOB = 6 kNm, ROP = 10 m/hour, and WOB = 98 kN

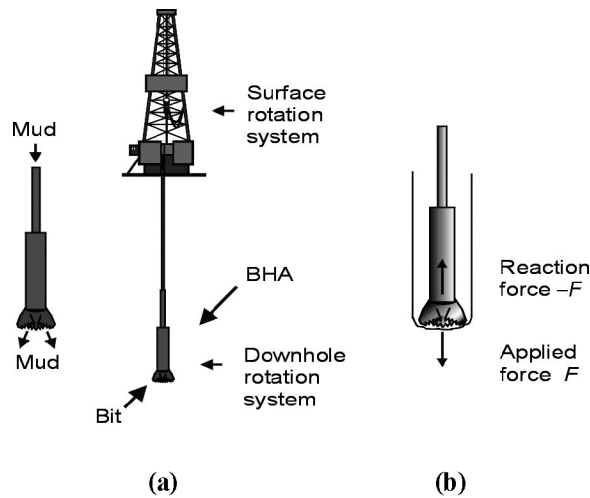


Figure 1. (a) Drilling rig and drill-string layout. The rotating bit at the bottom of the drill string fractures the rock. Rotation is imparted using a surface rotary system (rotary table or top drive) and/or (jointly or alone) downhole motors (or turbines) inserted in the bottom-hole assembly (BHA). Mud flows in the drill string, is ejected at the bit, and returns to the surface through the annulus. (b) Vertical (axial) force model of the drill bit source.

Table 1. Realistic ranges for drilling parameters.

Parameter	Minimum	Typical average	Maximum
Torque (Nm)	1000	3000–6000	15 000
rpm (rev/min)	60–80	120–180	500
WOB (kN)	0–1	100–200	300
ROP (m/h)	0–1	10	300

(10 tons), we obtain the total drilling power $W_{\text{drill}} = 75.4 + 0.272 \cong 75.7$ kW. In this example, total energy expended during one minute of drilling is ≈ 4.5 MJ and total energy expended during one hour of drilling (corresponding to 10 m of bit descent) is ≈ 272 MJ. Notice that the only term that contributes substantially to the drilling energy in equation 1 is the rotary power (first term on the right-hand side), which is transformed ultimately into the drilling action of the bit pushed against the rock by the weight on the bit.

When calculating the drill-bit power by equation 1, it is important to determine the downhole drilling parameters correctly. In general, surface measurements differ significantly from measurements made at the bit location (Falconer et al., 1989). The magnitude of surface torque can be several times the value of the downhole torque applied on the bit, and the downhole WOB may differ from the WOB calculated at the surface.

Energy losses for drill-string torque friction

In the rotary-drilling mode (i.e., with drill-string rotation), torque friction is the main cause of surface-power loss, and surface measurements are not representative of torque power at the bit. Torque loss is caused by friction between the rotating drill string and the wall of the borehole and by mud viscosity. The decay of torque in the rotating drill string can significantly alter the values of surface and downhole drilling energy. Where while-drilling downhole measurements (MWD) are not available, raw values of the downhole average energy can be estimated by calculating torque losses or by assuming approximate trends on the basis of experimental values for torque friction. In deviated wells, where side forces are important, torque loss may be determined using Coulomb's torque-friction coefficient η_{rot} — by definition, Coulomb's friction coefficient is the ratio of friction force over the normal force — defined as

$$\eta_{\text{rot}} = \frac{\text{TOR}_{\text{loss}}}{F_s \times r_{\text{DS}}}, \quad (2)$$

where TOR_{loss} is the torque loss over a drill-string element of radius r_{DS} , and F_s is the side force (such as the string-gravity component) pushing the element against the wall of the borehole. Values of the friction coefficient between 0.25 and 0.4 — which may correspond to cased- and open-hole conditions, respectively — are generally accepted (Lesage et al., 1988). In vertical wells, where side forces are assumed negligible, equation 2 is invalid for calculating torque losses caused by drill-string and bottom-hole-assembly (BHA) contacts with the wall of the borehole (see, for example, Poletto et al., 2001). In this case, torque losses may be estimated by relating reference measurements made at the surface (at the rotary motor) to those made downhole (at the bit) (Cunningham, 1968). Falconer et al. (1989) show an example in which the surface torque was twice the bit torque when a stabilizer entered a new, shallow formation drilled by a vertical well. Furthermore, in deep vertical wells, rotary friction effects caused by drilling-mud viscous damping are also important. Eronini et al. (1982) evaluated cases of reductions in torque by 75% for typical wells.

Effects of drag friction

Coulomb's drag-friction coefficient is defined as (Falconer et al., 1989)

$$\eta_{\text{drag}} = \frac{\text{WOB}_{\text{loss}}}{F_s}, \quad (3)$$

where WOB_{loss} is the weight loss for drag-friction effects over the drill-string element, subject to side force F_s . Weight losses for drag friction cause decreases in the effective WOB measured downhole relative to the WOB measured at the surface. This effect is important for deviated and horizontal wells. Falconer et al. (1989) measure while drilling the drag (also torque) loss over the drill string and calculate the average drag-friction coefficient from the MWD tool to the rotary table. This effect is generally less than 10% in the rotary mode (i.e., with drill-pipe rotation). However, static drag friction in the sliding mode (i.e., without drill-pipe rotation) is higher. In the static condition (sliding mode), drag friction may increase from less than 10% to 20–40% when a turbine or downhole motor is used without pipe rotation. This affects the calculation of the effective WOB and also can lead to a loss of SWD signal transmission through the drill string in vertical wells (Poletto and Miranda, 1998). Because the drilling energy expended by vertical-axial force is low when compared to the rotary energy (equation 1), the drag-friction effect can be considered negligible in computing the total energy expended for drilling. However, this effect cannot be considered negligible when the axial force actually exerted on the bit (WOB) is used to calculate the radiated energy, as we shall see.

Downhole motor drilling

When downhole positive-displacement motors (PDM) or turbines are used alone or in addition to surface-rotary drilling, the downhole rpm, hydraulic power, and efficiency to produce mechanical power can be obtained from their performance specifications. These are expressed as functions of mud's flow and specific gravity (Gabolde and Nguyen, 1999). Also, in this case, rotary power can be expressed in terms of torque and total rpm at the bit.

ENERGY REQUIRED TO DRILL A UNIT VOLUME OF ROCK

In the following section, I consider the energy required by the bit to drill the rock, disregarding energy losses caused by drill-string friction, as well as damping caused by the presence of drilling mud. The expended energy can be expressed by the concept of specific energy, which is used in drilling literature for bit selection (Rabia, 1985) and evaluation of drilling conditions. This concept can be defined in relation to the total drilling power given by equation 1 as

$$E_S = \frac{3600 \times W_{\text{drill}}}{A_B \times \text{ROP}}, \quad (4)$$

where A_B is the borehole area. E_S represents the energy required at the bit to drill a unit rock volume and has the physical dimensions of a stress. Pessier and Fear (1992) point out that the minimum (optimal) specific energy is reached when E_S is roughly equal to or approaches the compressive strength σ of the rock being drilled, which is defined as the strength at

which rock failure (as determined by laboratory triaxial loading tests) occurs. In other words, specific energy higher than σ should be related to energy dissipation and to a nonoptimal choice of drill bit for a given type of rock, or to the use of damaged and worn bits that produce low rates of penetration.

Simon (1963) analyzed the energy balance in percussive rock drilling and concluded that the expenditure of energy required to drill a unit volume of rock (i.e., E_S) is a quantity that varies from approximately 35 MPa to approximately 700 MPa. In his analysis, he assumes that the magnitude of this energy is roughly twice the compressive strength of the rock (as measured by a uniaxial loading test); he indicates also that it may range from roughly the same to several times the rock compressive strength, σ .

ENERGY BALANCE IN ROCK FRACTURE

Drilling energy is expended in different ways during the drilling process, and several effects are produced by a working bit. The principal and desired effect is breaking of the rock. Another effect is the emission of vibrations propagating in the surrounding formation, drilling plant, and borehole. Other effects are related to the dissipation of energy in the form of heat caused by the action of the drill bit and the friction of the pipes rotating in the borehole. The latter effect can be assumed negligible when considering only the friction of the rotating bit against the wall of the borehole (Falconer et al., 1988). Let W_{drill} be the total drilling power of equation 1. It can be represented as

$$W_{\text{drill}} = W_{\text{break}} + W_{\text{heat}} + W_{\text{vibr}}, \quad (5)$$

where W_{break} , W_{heat} , and W_{vibr} are the power used to generate the rock fragments, the heat dissipated, and the vibration power, respectively. The balance of energies involved in rock fracturing is discussed in detail by Simon (1963). In his analysis, Simon considers the following main energy requirements for fracturing rock.

New-surface energy (W_{break})

This is defined as the energy expended when a complementary pair of new free surfaces is formed. This energy corresponds to the work done against the cohesive forces that hold the material together. Simon uses Griffith's criterion (Jaeger, 1969) for brittle failure to calculate the new-surface energy involved in crack propagation under different tensile and compressive loading conditions. He estimates that this energy represents less than 1% of the total energy required to drill the rock. However, the evaluation of other authors indicates that this fraction is higher. For instance, Bernabe and Brace (1990) estimate it to be 1% to 10%, and Olgaard and Brace (1983) estimate the new-surface energy to be as much as 20% of the total energy (A. Gangi, personal communication, 2002). This effect is represented by W_{break} in power equation 5.

Elastic-strain energy (W_{heat})

Because it is impossible to give only the new-surface separation energy, "the best that can be done in practice is to apply repeated concentrated loadings on successive portions of the exposed rock at the bottom of the hole" (Simon, 1963,

p. 299). This action results in a system of distributed strain that would be favorable for breaking rock fragments. Somerton et al. (1961) use a photostatic system in laboratory tests to measure the permanent strain caused by cyclic loading on rock specimens drilled with roller bits. These researchers show that the stress/strain relations are nonlinear and dependent on past stress history and loading rate; consequently, the dynamic Young's moduli (of rocks altered by the cyclic loading) are substantially greater than Young's moduli determined by static tests.

By analyzing the different modes of tensile and compressive loading, Simon (1963) calculates that after failure has occurred, most of the elastic energy stored up to the point of failure is dissipated in "stress-wave initiated vibrations." He assumes that the rapid release of loads at the faces of the propagating crack following failure produces stress waves that are reflected back and forth between the fragments of the medium and soon dissipate into heat energy. So, despite the name "elastic strain" given by Simon (1963, p. 300) to this energy component, in my analysis this effect should contribute greatly to W_{heat} . Maurer (1965) analyzes friction in shear failure of rock under compression. Shear failure predominates in drilling because it is difficult to produce tensile stresses under the high compressive stresses of the earth. Friction in rock fractures produces heat — temperatures close to the melting temperature were measured at the rock fracture surface. It has to be stressed that the mechanical process of drilling requires the expenditure of heat-dissipated energy, which is "as necessary as . . . the new-surface energy," as Simon (1963) points out. Excess heat energy, which is affected by bit selection, hydraulics, pressure, and mechanical and drilling conditions, can be evaluated by using specific energy. Pessier and Fear (1992) suggest that excess heat generated per unit volume of removed rock is proportional to the difference in the specific energy E_S (equation 4) of two bits drilling at different E_S levels. The difference in heat energy per unit volume of drilled rock is

$$H = C(E_{S2} - E_{S1}). \quad (6)$$

If H and E_S are measured in cal/m^3 and pascal, respectively, we have $C = 0.239 \text{ cal/J}$. Pessier and Fear (1992) use specific energies $E_{S1} = 280 \text{ MPa}$ and $E_{S2} = 560 \text{ MPa}$ for two bits with diameters of $12\frac{1}{4} \text{ in.}$, both drilling at a penetration rate of 6 m/hour. We obtain a difference in drilling power of about 35 kW, which corresponds to a difference in heat drilling power [i.e., $H \times (\text{ROP}/3600) \times (\text{borehole area})$] of about 8370 cal/s. This amount of power, as pointed out by Pessier and Fear (1992), is certainly not negligible when compared to the total drilling power; see the example calculated after equation 1 in which the total power is 75 kW.

Stress waves produced in loading and unloading (W_{vibr})

In the title of this paragraph I have substituted the original term *dissipated* used by Simon (1963), with *produced*, because it defines the energy radiated out as stress waves in the far-field, that is, the drill-bit signal energy. It does not include the elastic energy temporarily stored in the near-field nor the energy of inelastic deformation in the rock close to the bit. Simon (1963) (see also Hunter, 1957) calculates the energy of the waves radiated for a concentrated loading on the surface

of a semi-infinite medium (horizontal half-space) to simulate the axial (vertical) action of a bit chisel struck by a weight. After Miller and Pursey (1954), Hunter (1957) calculates the radiation of energy in the form of elastic waves generated by a transient localized force acting normally to the free surface of a semi-infinite solid. This result is applied to the collision of a small body with the plane surface of a massive specimen in the Hertz equation, which takes no account of the dissipation of energy (see Love, 1944). Starting from Hunter's analysis, Simon (1963) calculates the total energy radiated during loading by integrating the power from zero up to the time t_0 at which the maximum loading force occurs. This gives

$$E_R = f_H(\nu) \frac{1}{Yc} \int_0^{t_0} \left(\frac{dF}{dt} \right)^2 dt, \quad (7)$$

where F is the loading force; $c = (Y/\rho)^{1/2}$ and Y are the theoretical thin-rod (bar) velocity and Young's modulus, respectively, of the rock of density ρ ; ν is the Poisson's ratio of the medium, and $f_H(\nu)$ is a function slowly varying with respect to ν , which can be expressed as

$$f_H(\nu) = \frac{2\beta(\nu)(1+\nu)}{\pi} \sqrt{\frac{1-\nu^2}{1-2\nu}}. \quad (8)$$

The function $f_H(\nu)$ approximatively equals 0.6 in a Poisson's medium, where $\nu = 0.25$ and $\beta(0.25) = 0.5347$ (see Hunter, 1957, equations 17 to 20). This theoretical calculation is performed by assuming that the dimensions of the region deformed inelastically are small compared with the dominant wavelength of the produced wave. By assuming the model of a dropping weight to simulate the indentation impact of a cone tooth, Simon (1963) shows that the ratio between radiated energy, E_R , and the impact energy, E_0 , during loading can be expressed as

$$\frac{E_R}{E_0} = f_H(\nu) \left(\frac{\pi^2}{2} \right) \left(\frac{K}{Y} \right) \left(\frac{l}{ct_0} \right), \quad (9)$$

where K is a constant of proportionality between force per unit chisel length versus displacement (it has the physical dimensions of a stress), and l is the length of the chisel edge. In his calculations, Simon (1963) assumes $(K/Y) \approx 10^{-2}$, $l = 1 \text{ in.}$, and $t_0 = 2 \text{ ms}$, and he obtains values on the order of 10^{-4} for the ratio E_R/E_0 between the energy radiated and the total energy of the loading process. Moreover, he estimates that the stress-wave energy produced on the unloading of a roller-cone tooth (see part 2 for a description of different bits) would be about three times higher than that resulting from the loading process. This difference is caused by the tooth moving out of engagement with the rock faster after a rock chip has been broken out as a consequence of the loading process, because it has a shorter distance to travel when disengaging. In his calculations, Simon (1963) assumes that the load force would be released more rapidly, $(dF/dt)^2$ would be nine times greater, t_0 three times smaller, and E_R should be about three times the energy radiated during loading. Similar values may be estimated when considering the simultaneous action of more teeth indenting the rock. For example, in a working roller bit, the number of rows of teeth N_T that bear the load at any one time is typically from 1 to 4 (Burgess and Lesso, 1985), and the total chisel length l consequently increases.

The basic concept of equation 7 is that the power radiated in the medium is proportional to the square of the instantaneous variation of the loading force F , i.e., $(dF/dt)^2$. This is a key point in understanding the behavior of the drill-bit source and, in general, of vibrating sources. From this concept, it follows that another force having equal maximum magnitude of F and acting with twice the rate in a time interval of half the duration produces double radiated energy. In other words, for equal maximum magnitude, high-frequency, abrupt, and irregular discontinuous changes are more important than regular and slow periodic action of the bit force. The structure and drilling action of roller-cone bits, as well as of polycrystalline diamond compact (PDC) bits, is described in more detail in part 2 of this paper, in Hardage (1992) for SWD with roller-cone bits, and in the drilling literature (e.g., Bourgoyne et al., 1991; Devereux, 1999). Analysis of the theoretical forces for an idealized roller bit shows that the chipping action of the teeth wedges is a primary cause of discontinuity of vertical, horizontal, and torque forces when a tooth moves out of contact with the rock (Biggs et al., 1969). Examples of unloading rates, which are about 5 times faster than loading rates, are shown by Sheppard and Lesage (1988), who measure the forces at the teeth of a drilling roller-cone bit. In these conditions, higher unloading energy ratios, on the order of 10^{-3} , can be expected. After Simon (1963), several other authors calculate theoretically and analyze the kinematic and dynamic behavior of drill bits using laboratory and field measurements. These results are analyzed in part 2 of this paper, which describes the performance of different types of drill bits.

Finally, Simon (1963) calculates that, during the sporadic propagation of rock cracks, E_R/E_0 can be 0.1, or closer to unity, and that high-frequency energy is involved during these “catastrophic” events. This high-frequency energy accounts for the local-heat dissipation of elastic-strain energy. He concludes that the energy of the radiated waves is a negligible fraction of the total energy and does not substantially affect drilling efficiency. Table 2 summarizes Simon’s (1963) results. However, these results may be underestimated in the evaluation of new-surface energy, which may be, if we assume the opinion of other authors, 10% or more of the total drilling energy expended by the bit.

For SWD purposes, we have to determine the contribution of total energy expended during long drilling intervals, such as those used for SWD acquisition. This total energy can be very high. Hence, the low relative value of drill-bit energy radiated into stress waves becomes important, and its cumulative contribution is comparable to that of conventional seismic sources. In our analysis, the energy of the waves radiated into the rock contributes to W_{vibr} . Simon’s (1963) results in equa-

tions 7 and 9 include only (body and surface) waves radiated into the rock, and they are in agreement with the analysis of impedances, for which — with equal excitation force F — the energy radiated into the rock decreases in the presence of hard rocks, i.e., with high values of Yc in equation 7. However, we must take into account that the previous results are calculated for a source acting on a free surface, not for a source buried in an infinite, unbounded medium. It can be shown that, if we assume a harmonic force in equation 7, and using equation 8 we calculate the radiated power over a loading period, we obtain the same total power (given by $\eta = 4.836$ in equation 23 of part 2) as calculated by Miller and Pursey (1954) for radiation from a pulsating vibrator plate (with uniform stress over the baseplate) at the surface of Poisson’s half-space (Cassand and Lavergne, 1971, p. 206). Furthermore, Simon’s (1963) analysis does not include the significant part of the energy transmitted into the drill string and borehole. We will see later that partitioning of the energy produced by the drill-bit displacement source in the form of waves radiated into the rock and drill string is related to the reflection coefficient at the bit-rock interface. This ratio is important for characterizing SWD signals because the energy level of the SWD data is commonly obtained by geometric averaging of the coherent energy measured in the rock and drill string.

DOWNHOLE RADIATION (INFINITE MEDIUM)

To quantify the downhole bit–seismic-source energy, I develop here the analysis of downhole vibrations in the rock (infinite-medium approximation) and in the drill string as produced by a downhole force. The purpose is to compare the radiated field to the vibration levels measured in the drill string. The drilling literature provides several examples of theoretical calculations and experiments performed to measure drill-bit forces. To take into account the dynamic behavior of the bit, I have reformulated the half-space expression for the radiated energy equation 7 on the basis of the drill-bit radiation pattern in an unbounded, infinite, homogeneous, and isotropic medium (Gangi, 1987). Assume, without loss of generality, vertical drilling, and for simplicity, let the force exerted by the bit be represented by the harmonic vertical component

$$F = F_0 \sin \omega t, \quad (10)$$

where $\omega = 2\pi/T$ is the angular frequency. In this approximation, I have not accounted for the gouging torsion; i.e., the SH component measured, for instance, by Sheppard and Lesage (1988) and Lesage et al. (1988), and included in the calculation of the roller-bit radiation pattern by Rector and Hardage (1992) and, in finely stratified media, by Carcione and Carrion (1992). Nor have I accounted for the lateral-force components (Langeveld, 1992) of the point source (see part 2 of this paper) and flexural borehole and string waves.

Now, consider an unbounded, homogeneous, and isotropic medium in which a buried vertical force F given by equation 10 acts. The vertical-force model was proposed by Rector and Hardage (1992) to calculate the radiation pattern of a working roller-cone bit. This is a simplified source model, and I have used the same approach here to calculate the far-field power radiated in the formation (Figure 1b). Moreover, I have assumed a vertical-reaction-force source to calculate the power

Table 2. Simons’s (1963) drilling-energy balance (source at the surface).

Type of energy expenditure	Fraction (%)
New surface	~1
Elastic strain into local (“necessary”) heat	~99
Radiation (far-field)	~ 10^{-4}
Total	100

transmitted into the drill string in the form of one-dimensional axial waves and to calculate the partition of these energies.

Let us consider a wave $f = f(\omega t - kr)$ radiated in the far-field with velocity $c = \omega/k$, where ω is the radiation frequency, $k = 2\pi/\lambda$ is the wavenumber, λ is the wavelength, and r is the radial distance from the point source. The far-field and near-field concepts are explained by, for instance, Aki and Richards (1980). The far-field approximation holds when $r \gg c/\omega$ (or $kr \gg 1$), in which case the near-field and intermediate-field terms — which decrease as $1/r^3$ and $1/r^2$, respectively — become negligible. Rector and Hardage (1992) use the expressions proposed by White (1965) [see also, Love (1944)] to represent, in a point located in the far-field, the displacement produced by a vertical force of time-law $F(t) = F_0 f(t)$, where F_0 is a constant magnitude. The displacement components are given in spherical coordinates as

$$\begin{aligned} u_r &= \frac{F_0 \cos \phi}{4\pi\rho\alpha^2 r} f\left(t - \frac{r}{\alpha}\right), \\ u_\theta &= 0, \\ u_\phi &= -\frac{F_0 \sin \phi}{4\pi\rho\beta^2 r} f\left(t - \frac{r}{\beta}\right), \end{aligned} \quad (11)$$

where ϕ is the angle between the radius and the vertical axis, θ is the azimuth angle (Figure 2), and α and β are the velocities of compressional and shear waves in the formation of density ρ . As pointed out by Rector and Hardage (1992), the displacements u_r and u_ϕ represent the P and SV components, respectively. Using the time-harmonic force of equation 10, we obtain

$$\begin{aligned} u_r &= \frac{F_0 \cos \phi}{4\pi\rho\alpha^2 r} \sin \omega\left(t - \frac{r}{\alpha}\right), \\ u_\phi &= -\frac{F_0 \sin \phi}{4\pi\rho\beta^2 r} \sin \omega\left(t - \frac{r}{\beta}\right). \end{aligned} \quad (12)$$

Let the particle velocity be $v = \partial u / \partial t$. The amount of energy transmitted per unit time across the unit area normal to the wave direction of propagation (i.e., the energy flux) of a wavefront radiated with propagation velocity c_w is given by $P_w = \rho c_w v^2$ (Aki and Richards, 1980). This assumption holds for harmonic waves propagating spherically in the far-field

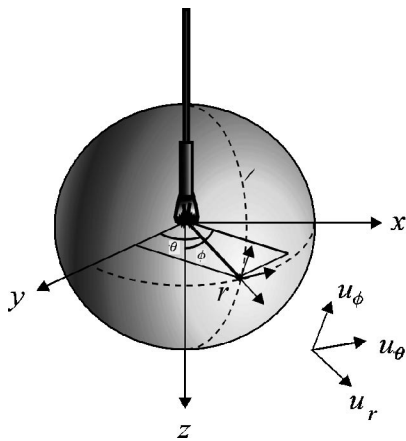


Figure 2. System of spherical coordinates used to represent spherical waves propagating from the bit. The vertical (or drilling) axis is z .

condition $kr \gg 1$. We are interested not in the instantaneous power, which depends on the instantaneous sine phase, but in the intensity obtained by averaging the power flux per unit surface over a period $T = 2\pi/\omega$. The average energy fluxes are given for radial P and tangential SV components, respectively, by

$$\begin{aligned} \bar{P}_r &= \frac{1}{T} \int_0^T \rho\alpha v_r^2(t) dt = \frac{1}{2} \rho\alpha V_r^2, \\ \bar{P}_\phi &= \frac{1}{T} \int_0^T \rho\beta v_\phi^2(t) dt = \frac{1}{2} \rho\beta V_\phi^2, \end{aligned} \quad (13)$$

where

$$\begin{aligned} V_r(\phi) &= \frac{\omega F_0 \cos \phi}{4\pi\rho\alpha^2 r}, \\ V_\phi(\phi) &= \frac{\omega F_0 \sin \phi}{4\pi\rho\beta^2 r}, \end{aligned} \quad (14)$$

and where I have used the relations

$$\begin{aligned} \frac{1}{T} \int_0^T \cos^2 \omega\left(t - \frac{r}{\alpha}\right) dt &= \frac{1}{T} \int_0^T \cos^2 \omega\left(t - \frac{r}{\beta}\right) dt \\ &= \frac{1}{2}. \end{aligned} \quad (15)$$

Displacement and power-flux radiation patterns are shown in Figure 3. The integrals of equation 15 depend on the square of the time derivative of the force. In this case, the force is sinusoidal, and the integrals equal 0.5. (However, we will see in part 2 of this paper that by using a realistic indentation force, the integral can equal 1.5, i.e., three times higher.) The mean value of the total energy flux during a period T , i.e., the total average power radiated in the far-field (Kaufman and Levshin, 2000, p. 179), is calculated by integrating the intensity of P- and SV-waves over the spherical surface of a wavefront with an arbitrary radius r , so that we can take as large a value for r

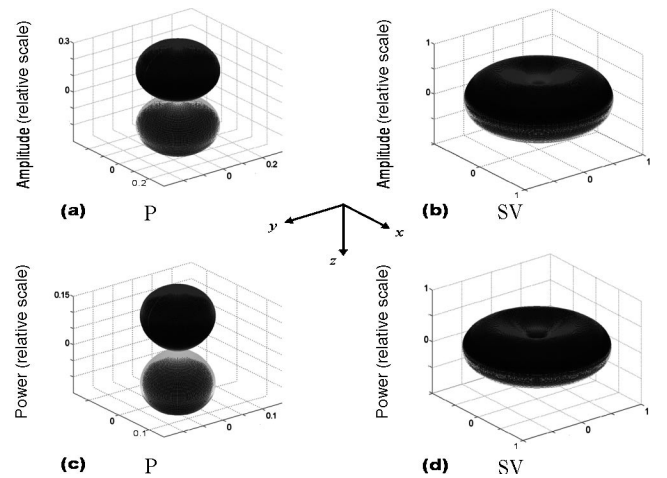


Figure 3. Far-field radiation properties calculated assuming a Poisson's medium (i.e., where $\alpha^2 = 3\beta^2$). Compressional P- and shear SV-wave displacements are shown with the same relative scale in Figures 3a and 3b, respectively. Compressional P- and shear SV-wave power fluxes are shown with the same relative scale in Figures 3c and 3d, respectively.

as desired in order to satisfy the far-field condition $kr \gg 1$. We obtain

$$\begin{aligned} W_r &= \int_S \bar{P}_r(\theta, \phi) r^2 \sin \phi \, d\theta \, d\phi \\ &= \frac{1}{2} \rho \alpha r^2 \int_0^{2\pi} d\theta \int_0^\pi V_r^2(\phi) \sin \phi \, d\phi, \\ W_\phi &= \int_S \bar{P}_\phi(\theta, \phi) r^2 \sin \phi \, d\theta \, d\phi \\ &= \frac{1}{2} \rho \beta r^2 \int_0^{2\pi} d\theta \int_0^\pi V_\phi^2(\phi) \sin \phi \, d\phi, \end{aligned} \quad (16)$$

which gives, for compressional P- and shear SV-waves,

$$\begin{aligned} W_r &= \frac{1}{6} \frac{\omega^2 F_0^2}{4\pi \rho \alpha^3}, \\ W_\phi &= \frac{1}{3} \frac{\omega^2 F_0^2}{4\pi \rho \beta^3}. \end{aligned} \quad (17)$$

INTEGRATED DOWNHOLE-RADIATION IMPEDANCE

The impedance that a medium presents to a given motion is a measure of the amount of resistance to particle motion (Aki and Richards, 1980, p. 137). By definition, the radiation impedance in elasticity is the ratio of stress to particle velocity. In the far-field, it equals the acoustic impedance $\rho\alpha$ and $\rho\beta$ for P- and SV-waves, respectively. If the radiation impedance is complex, its real and imaginary parts are also called specific acoustic resistance and reactance, respectively.

Because we are interested in the total powers radiated both in the formation and in the drill string, we introduce integrated impedances. Here, the term “total power” has the meaning of integrated over the whole surface (of the spherical surface in the formation or cross section in the drill string). To express the radiated power in term of integrated resistance of the formation to radiation at a given harmonic frequency, I have reformulated equations 17 by introducing an equivalent, “effective” radiation radius, which is defined for the compressional P- and SV-shear waves by

$$\begin{aligned} R_\alpha^2 &= \frac{1}{I_\alpha k_\alpha^2}, \\ R_\beta^2 &= \frac{1}{I_\beta k_\beta^2}, \end{aligned} \quad (18)$$

where $k_\alpha = \omega/\alpha$ and $k_\beta = \omega/\beta$. I_α and I_β are the normalized surface integrals of the unit energy-flux patterns calculated as

$$\begin{aligned} I_\alpha &= \frac{1}{4\pi} \int_0^{2\pi} d\theta \int_0^\pi \cos^2 \phi \sin \phi \, d\phi = \frac{1}{3}, \\ I_\beta &= \frac{1}{4\pi} \int_0^{2\pi} d\theta \int_0^\pi \sin^2 \phi \sin \phi \, d\phi = \frac{2}{3}. \end{aligned} \quad (19)$$

It can be observed that the equivalent radii R_α and R_β are of the same order of magnitude (of the dominant wavelength) as the reference radii ($r = k_\alpha^{-1}$ and $r = k_\beta^{-1}$) used to define the limits between near- and far-field for compressional and shear waves, respectively. By using R_α and R_β the integrated impedances can be expressed by the product of the radiation impedances (or far-field impedances) and the effective areas

$A_\alpha = 4\pi R_\alpha^2$ and $A_\beta = 4\pi R_\beta^2$. We have

$$\begin{aligned} Z_\alpha &= A_\alpha \rho \alpha = \frac{12\pi \alpha^3 \rho}{\omega^2}, \\ Z_\beta &= A_\beta \rho \beta = \frac{6\pi \beta^3 \rho}{\omega^2}, \end{aligned} \quad (20)$$

for the downhole P and SV radiated signals, respectively. The integrated impedances of equations 20 have the dimension of force over particle velocity (while the radiation impedance has the dimension of stress over particle velocity). The variation of the integrated radiation impedances with frequency ($Z_\alpha, Z_\beta \propto \omega^{-2}$) is in agreement with the average radiation impedance curves as calculated for a surface vibroseis source by Baeten and Ziolkowski (1990). Hence, equations 17 can be expressed in terms of force and global impedance as

$$\begin{aligned} W_r &= \frac{F_0^2}{2} \frac{1}{Z_\alpha}, \\ W_\phi &= \frac{F_0^2}{2} \frac{1}{Z_\beta}. \end{aligned} \quad (21)$$

The form of equations 21 is preferable for comparing the impedances of the radiated and drill-string energy because the characteristic impedance in one-dimensional drill strings is defined as the ratio of force over particle velocity, rather than stress over particle velocity. Equations 17 are preferable for calculating the power radiated by a known periodic force.

Total P + SV power radiated in the formation

The total power radiated in the formation is obtained by the sum of the compressional- and shear-radiated powers as

$$W_R = W_r + W_\phi = \frac{1}{6} \frac{\omega^2 F_0^2}{4\pi \rho} \left(\frac{1}{\alpha^3} + \frac{2}{\beta^3} \right). \quad (22)$$

In terms of total radiation impedance, we have

$$W_R = \frac{F_0^2}{2} \frac{1}{Z_R}, \quad (23)$$

where the total impedance is given by

$$\frac{1}{Z_R} = \frac{1}{Z_\alpha} + \frac{1}{Z_\beta}. \quad (24)$$

Assuming a Poisson's medium, denoted by superscript ^(P), we have $(\alpha/\beta) = \sqrt{3}$, and

$$W_R^{(P)} = \frac{1}{6} \frac{\omega^2 F_0^2}{4\pi \rho \alpha^3} (1 + 6\sqrt{3}). \quad (25)$$

In this case, the total P + SV radiated power produced by a downhole sinusoidal force can be written as

$$W_R^{(P)} = \frac{F_0^2}{2} \frac{1}{Z_R^{(P)}} \approx 0.151 \frac{\omega^2 F_0^2}{\rho \alpha^3}, \quad (26)$$

where

$$Z_R^{(P)} = \frac{12\pi \rho \alpha^3}{\omega^2 (1 + 6\sqrt{3})} \approx \frac{1}{0.302} \frac{\rho \alpha^3}{\omega^2} \quad (27)$$

is the radiation impedance calculated for the given Poisson's medium and frequency. Compared with equation 23 of part 2, calculated for total radiation from a surface force, equation 26

could be roughly interpreted in the following way: a given excitation force energizes the half-infinite medium with approximately twice the radiated power than the infinite one. From equation 25, it follows that the total average compressional P power is about 10% of the total radiated power. However, when averaging the compressional power value of equation 17 over the spherical wavefront of area $4\pi r^2$ (in order to compare it with the power of a pressure source of a spherical radiation pattern), remember that the radiation power of the P component produced by the force in the directions of the maximum radiation (i.e., $\phi = 0, \pi$) is three times its average power density. A comparison between drill-bit and conventional sources is contained in part 2 of this paper. In the direction of maximum radiation, the maximum compressional power density at radius r is

$$P_r^{(\max)} = \frac{1}{32\pi^2 r^2} \frac{\omega^2 F_0^2}{\rho \alpha^3}. \quad (28)$$

Radiation from a nonsinusoidal force

In general, when assuming a force of arbitrary time law $F(t)$ acting in the time interval $(0, T)$, we have to calculate the integrals

$$I_f = \frac{1}{T} \int_0^T \left(\frac{\partial F}{\partial t} \right)^2 dt, \quad (29)$$

and multiply the previous power results by the scaling factor $2I_f(F_0\omega)^{-2}$.

NEAR-FIELD EFFECTS (AND COMPLEX INTEGRATED IMPEDANCE)

Near-field energy consists of temporarily stored energy and radiated energy. The radiated energy is the same as the far-field energy. If we want to look at radiated energy at the geophone traces, we need only the far-field. However, the near-field effects are important to calculate pilot vibrations and the

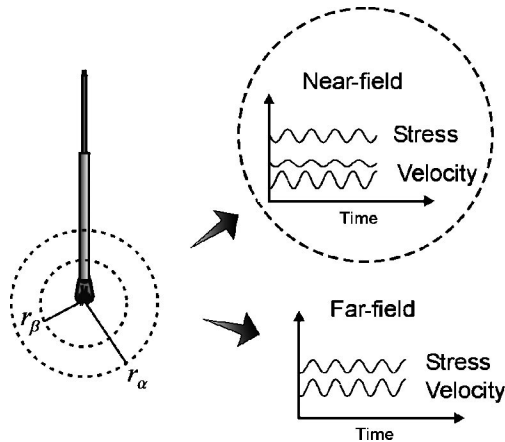


Figure 4. The radii $r_\alpha = 1/k_\alpha$ and $r_\beta = 1/k_\beta$ define the near-field/far-field for compressional and shear waves radiated spherically from the bit. Assuming $f = 30$ Hz, $\alpha = 4200$ m/s, $\beta = 2425$ m/s, we obtain $r_\alpha \sim 22$ m, and $r_\beta \sim 13$ m. In the near-field, particle velocity is the sum of components that are in- and out-of-phase with stress. In the far-field, stress and particle velocity are in phase.

exchange of energy with the drill string, where a reference pilot signal can measure propagating and stationary waves. Moreover, to relate the rotary-drilling equations to the vibrations in the formation close to the bit, we need to account for the near-field effects. In fact, while the far-field terms dominate in the far-field, the near-field terms are important in the near-field (Aki and Richards, 1980, p. 119)(Figure 4). The general expression of the total — near- and far-field — particle displacements produced by a single vertical force $F_0 f(t)$ in an unbounded, isotropic, elastic solid is given as (White, 1965, p. 214)

$$u_r^T = \frac{F_0 \cos \phi}{4\pi \rho r \alpha^2} \left[\frac{2\alpha^2}{r^2} \int_{r/\alpha}^{r/\beta} t' f(t-t') dt' + f\left(t - \frac{r}{\alpha}\right) \right],$$

$$u_\phi^T = \frac{F_0 \sin \phi}{4\pi \rho r \beta^2} \left[\frac{\beta^2}{r^2} \int_{r/\alpha}^{r/\beta} t' f(t-t') dt' - f\left(t - \frac{r}{\beta}\right) \right], \quad (30)$$

for radial P and tangential SV displacement waves, respectively. Assuming a harmonic force $f(t) = \sin \omega t$ at the bit and integrating previous equations (Love, 1944, p. 306), after some calculations, we have (see also Pilant, 1979, p. 79)

$$u_r^T = R_0(R_1 \sin \omega \xi_\alpha + R_2 \cos \omega \xi_\alpha + R_3 \cos \omega \xi_\beta + R_4 \sin \omega \xi_\beta),$$

$$u_\phi^T = S_0(S_1 \sin \omega \xi_\beta + S_2 \cos \omega \xi_\beta + S_3 \cos \omega \xi_\alpha + S_4 \sin \omega \xi_\alpha), \quad (31)$$

where $\xi_\alpha = (t - \frac{r}{\alpha})$ and $\xi_\beta = (t - \frac{r}{\beta})$. The coefficients R_i and S_i ($i = 0, 1, 2, 3, 4$) are given in Appendix A. Note that only R_0 and S_0 depend on the angle ϕ and do not depend on the frequency ω . In the far-field, $R_1 = 1$ and $S_1 = -1$, while the terms with higher index are zero. Equations 31 can be rewritten in terms of orthogonal sine and cosine harmonics as

$$u_r^T = R_0(Q_1 \sin \omega t + Q_2 \cos \omega t),$$

$$u_\phi^T = S_0(Q_3 \sin \omega t + Q_4 \cos \omega t), \quad (32)$$

where the coefficients Q_i are given in Appendix A. For the near-field condition ($k_\alpha r < k_\beta r \ll 1$), the amplitude of the sine over the cosine components Q_1/Q_2 and Q_3/Q_4 for radial and transverse components, respectively, have large values. Expanding the terms in powers of $k_\alpha r$ and $k_\beta r$, it can be shown that in a Poisson's medium (Figure 5) (Appendix A)

$$\lim_{k_\alpha r \rightarrow 0} \left| \frac{Q_1}{Q_2} \right| = \frac{9}{k_\alpha r (1 + 6\sqrt{3})} \gg 1,$$

$$\lim_{k_\alpha r \rightarrow 0} \left| \frac{Q_3}{Q_4} \right| = \frac{6}{k_\alpha r (1 + 6\sqrt{3})} \gg 1. \quad (33)$$

Near-field axial displacement

If the single-force model is assumed to represent the bit source at a point, $r = 0$ is a singularity for displacement. Because the real bit is not a point, I integrate the contribution of the force distributed over its face. The knowledge of the exact distribution of forces at the bit face is, in general, not

available (Ma et al., 1995). To calculate the near-field effect, I use the averaged (over the bit area) force, and assume that the source is distributed uniformly over $0 < r < r_b$, where r_b is the bit radius (that is, an ideal flat-bit model). Using equations 33 to calculate the phase of the harmonic displacements, it can be shown that the ratios Q_1/Q_2 and Q_3/Q_4 may be on the order of 10^2 at $r = r_b$ for realistic bits and formation properties and for frequencies ranging between about 15 to 50 Hz. A comparable result can be obtained by calculating the axial displacement at distance h in front of the bit, which is assumed to be flat and subject to uniform axial stress distribution:

$$\sigma_0 = \frac{F_0}{A_b} \sin \omega t, \quad (34)$$

over the bit area $A_b = \pi r_b^2$. In this approximation, I integrate the contribution of the elementary areas to obtain the integrated axial displacement at a point on the bit axis at distance h from the bit face (Figure 6):

$$\begin{aligned} \hat{u} &= \int u_z dA = \int_0^{2\pi} d\theta \int_0^{r_b} (u_r \cos \phi - u_\phi \sin \phi) \xi d\xi \\ &= \Gamma_1 \sin \omega t + \Gamma_2 \cos \omega t, \end{aligned} \quad (35)$$

where ξ and ϕ are the radial and angular variables of Figure 6, and the coefficients Γ_i are calculated separately for sine- and cosine-wave components as

$$\begin{aligned} \Gamma_1 &= \frac{2\pi}{A_b} \int_0^{r_b} (R_0 Q_1 \cos \phi - S_0 Q_3 \sin \phi) \xi d\xi, \\ \Gamma_2 &= \frac{2\pi}{A_b} \int_0^{r_b} (R_0 Q_2 \cos \phi - S_0 Q_4 \sin \phi) \xi d\xi, \end{aligned} \quad (36)$$

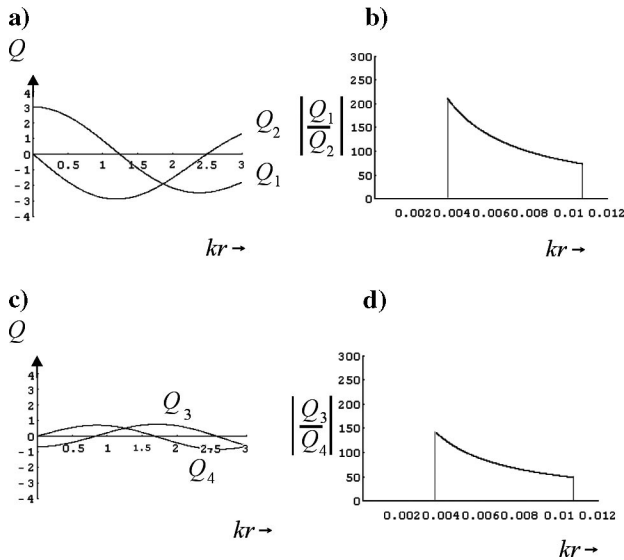


Figure 5. (a) Amplitude of Q_1 and Q_2 near-field radial displacement components as $k_\alpha r \rightarrow 0$ in a Poisson's medium; (b) ratio of $-Q_1/Q_2$ calculated for realistic formation and $r = r_b$ and frequencies ranging from 16 to 46 Hz. (c) Amplitude of Q_3 and Q_4 near-field radial displacement components as $k_\alpha r \rightarrow 0$. (d) Ratio of $-Q_3/Q_4$.

where I used equation 34. It can be shown that

$$\begin{aligned} \lim_{h \rightarrow 0} \Gamma_1 &= C_0 r_b, \\ \lim_{h \rightarrow 0} \Gamma_2 &= -C_0 r_b \frac{k_\alpha r_b (1 + 6\sqrt{3})}{12}, \end{aligned} \quad (37)$$

where $C_0 = F_0/(A_b \rho \alpha^2)$ and where I have used the near-field approximation for the coefficients Q_i and the fact that the approximations of Q_2 and Q_4 depend on r (Appendix A). We have

$$\lim_{h \rightarrow 0} \left| \frac{\Gamma_1}{\Gamma_2} \right| = \frac{12}{k_\alpha r_b (1 + 6\sqrt{3})} \gg 1. \quad (38)$$

The integrated result in equation 38 is obtained at the bit face ($h \rightarrow 0$) and is of the same order as those we obtain if we use $r = r_b$ in equations 33 for a point force. In other words, the axial displacement at a position very close to the bit source has a phase close to that of the force, as it is composed of a sine wave of magnitude $|\Gamma_1| (\gg |\Gamma_2|)$ and a cosine wave of magnitude $|\Gamma_2| (\ll |\Gamma_1|)$. The phase of the near-field axial displacement is

$$\varphi(\omega, \alpha, r_b) = \arctan \left[-\frac{12}{k_\alpha r_b (1 + 6\sqrt{3})} \right] \approx -\frac{\pi}{2}, \quad (39)$$

for seismic frequencies ($k_\alpha r_b \sim 100^{-1}$). This gives

$$\cot \varphi = -\frac{k_\alpha r_b (1 + 6\sqrt{3})}{12} \approx -0.95 k_\alpha r_b, \quad (40)$$

with $\cot \varphi \approx \cos \varphi$ for $k_\alpha r_b \ll 1$. The phase φ is used in the following to calculate in- and out-of-phase stress-velocity relations.

Energy flux and near-field effects

The phase φ determines the magnitude of vibrations in-phase and out-of-phase with force. This analysis is used to determine not only the radiated energy (far-field waves) but also the energy interchanged between the formation and the bit (as part of the drill string) for near-field effects. The particle velocity in terms of sine and cosine waves in the near field is

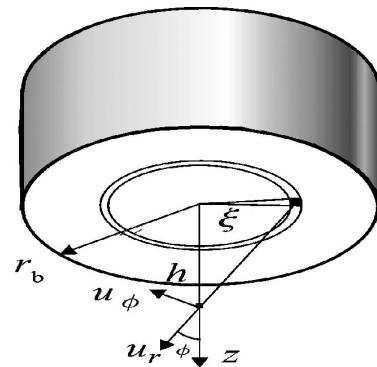


Figure 6. System of coordinates used to calculate displacement in front of an ideal flat bit: ξ is the radial distance from bit center and h is the distance of the point ahead of the bit in which the axial contribution from radial and tangential components is summed.

given by (equation 33)

$$\begin{aligned} v_r &= \frac{\partial u_r}{\partial t} = \omega R_0(Q_1 \cos \omega t - Q_2 \sin \omega t) \\ &\approx \omega R_0 Q_1 \cos \omega t, \\ v_\phi &= \frac{\partial u_\phi}{\partial t} = \omega S_0(Q_3 \cos \omega t - Q_4 \sin \omega t)v_\phi \\ &\approx \omega S_0 Q_3 \cos \omega t, \end{aligned} \quad (41)$$

while in the far-field ($k_\alpha r \gg 1$), we obtain again the propagating waves of equations 12. The integrated axial velocity is calculated from equation 35 as

$$\hat{v} = \frac{\partial \hat{u}}{\partial t} = \omega \Gamma_1 \cos \omega t - \omega \Gamma_2 \sin \omega t. \quad (42)$$

From equations 37 we have

$$v_0 = \lim_{h \rightarrow 0} \hat{v} = \frac{F_0 k_\alpha r_b}{A_b \rho \alpha} \left[\cos \omega t + \frac{k_\alpha r_b (1 + 6\sqrt{3})}{12} \sin \omega t \right]. \quad (43)$$

We can calculate the instantaneous energy flux at the bit axis using

$$\sigma_0 v_0 = \frac{F_0^2 k_\alpha r_b}{A_b^2 \rho \alpha} (\cos \omega t \sin \omega t - \cot \varphi \sin^2 \omega t), \quad (44)$$

where I have used equations 34 and 40. To determine the work done by the source, I multiply by the bit area and average over a period $T = 2\pi/\omega$ to obtain the average power:

$$A_b \overline{\sigma_0 v_0} = -\frac{F_0^2 k_\alpha r_b}{2A_b \rho \alpha} \cot \varphi = W_R^{(P)}, \quad (45)$$

which equals the total radiated power in a Poisson's medium (equation 25). Only the second — and very small amplitude — term of equation 44 contributes, on average, to energy expenditure; this is the energy of the far-field wave radiation. Contrarily, the $\cos \omega t$ component of particle velocity is orthogonal to the force, which has a $\sin \omega t$ time dependence. The contribution of this component to the average power over a period T is zero. This near-field term has higher amplitude and represents the energy continuously and locally interchanged between source and formation.

Complex integrated impedance

I reformulate the definition of the integrated impedance to include the near-field effects. Because the stress in the proximity of the bit is a sine wave (see also Somerton et al., 1961), to obtain particle velocity by superposition of sine and cosine waves, a complex impedance has to be used (Lutz et al., 1972; Clayer et al., 1990). In Appendix B, I calculate the complex near-field integrated impedance over the bit area (using the σ_0 and v_0 complex) as

$$Z_b = \frac{A_b \sigma_0}{v_0} = -\frac{A_b \rho \alpha}{k_\alpha r_b} (\cos \varphi \sin \varphi + i \sin^2 \varphi), \quad (46)$$

and relate the near- and far-field integrated impedances. The total integrated impedance of equation 27 can be expressed as

$$Z_R^{(P)} = -\frac{A_b \rho \alpha}{k_\alpha r_b} \tan \varphi, \quad (47)$$

which gives

$$Z_b = Z_R^{(P)} (\cos^2 \varphi + i \cos \varphi \sin \varphi). \quad (48)$$

Note that the real part of the acoustic impedance of equation B-7 is close to the impedance at the bit ($A_b \rho \alpha$), as calculated by Poletto et al. (2000) in the plane-wave approximation without accounting for the complex near-field effects.

ENERGY BALANCE IN TERMS OF DRILLING PARAMETERS

Assuming that the interacting process between a bit and rock during drilling is a stable random process (Ma et al., 1995), one way to obtain information about the expended energy is to relate the average drilling action and the main drilling parameters. Falconer et al. (1988) introduce dimensionless drilling parameters as diagnostic indicators to separate the lithology effects from drilling mechanics data. These are the dimensionless downhole torque and rate of penetration, defined as:

Dimensionless torque

Rotary drilling converts the load on the bit into indentation and gouging forces that produce a momentum of torque resistance to rotation proportional to the bit diameter. Hence, the dimensionless torque is defined as

$$T_D = \frac{\text{TOR}}{\text{WOB} \times D}, \quad (49)$$

where $D = 2r_b$ is the bit and borehole diameter.

Dimensionless rate of penetration

The rate of penetration is ideally proportional to the bit rotary speed, rpm, and the dimensionless rate of penetration is defined as

$$R_D = \frac{\text{ROP}}{\text{rpm} \times D}. \quad (50)$$

Falconer et al. (1988) analyzed the torque drilling model by adopting an energy-balance approach, calculating the relation between the work per revolution produced by the downhole torque and the vertical (axial) distance x_p penetrated and gouged by the bit. They assumed that the friction of the borehole walls against the rotating bit is negligible. To evaluate the relation between vertical force and rotary drilling, they assume that the force F per unit width needed to push a sharp tooth into the rock is proportional to the maximum cross-sectional area embedded in the rock, hence

$$F(x_p) = \sigma_p \tan \Theta x_p, \quad (51)$$

where x_p is the depth of penetration and Θ is the tooth semian- gle for roller-cone bits, or the rake angle (see part 2) for polycrystalline diamond compact (PDC) bits. The constant σ_p has the dimension of a stress that represents the in-situ rock hardness (or penetration strength, not to be confused with rock strength as calculated by uniaxial load tests; however, the authors have pointed out that it can have an equivalent meaning in brittle fracturing). The work done vertically by an indentation

force is calculated by integrating $F(x_p)$ from 0 to x_p and is proportional to x_p^2 . The work of the transverse gouging action is assumed proportional to depth penetration x_p . The total torque energy per unit revolution frequency (i.e., $\omega_{rev} = 2\pi$) can be expressed as the sum of the gouging and indentation terms

$$2\pi \text{TOR} = b_4 \times \tau x_p D^2 + b_5 \times \sigma_p x_p^2 D, \quad (52)$$

where b_4 and b_5 are constants used by the authors and depend on the bit properties and number of impacts per revolution. The constant τ has the dimension of a stress and represents the in-situ rock shear strength. The first term, linear in x_p on the right side of equation 52, corresponds to the work expended in gouging. The second term, quadratic in x_p , corresponds to the work expended in pushing the bit teeth into the formation in a single revolution. The frequency of the torque energy per unit revolution of equation 52 can be rewritten in implicit form with respect to x_p and in terms of the dimensionless drilling parameters given by equations 49 and 50 as

$$T_D = b_6 \times (\tau/\sigma_p) + b_8 \times R_D^{1/n}, \quad (53)$$

where b_6 and b_8 are dimensionless constants of proportionality used by Falconer et al. (1988). The constants b_6 and b_8 account for the gouging and indenting bit action, respectively. The integer n relates the dimensionless rate of penetration to x_p , being $T_D \propto (x_p/D)^n$. Usually, n is equal to 1 or 2, depending on the average crater geometry (possible superposition of craters created by different teeth). Equation 53 is assumed valid both for roller-cone and PDC bits. The constants b_6 and b_8 have been discussed in detail by the authors. For instance, the indentation coefficient can be assumed to be $b_8 = 0.08$ for a milled-tooth roller cone (see part 2). Because dimensionless torque and rate of penetration can be measured, it follows from equation 53 that it is possible to calculate the relative value of vertical (or axial) indentation energy with respect to the total rotary energy (T_D). In general, the second (indentation) term is small compared to the first (gouging) term of the torque equation. Once the penetration energy involved in rock fracturing has been calculated, we have to calculate which part of the work done by the vertical-axial force corresponds to elastic radiated energy.

Sheppard and Lesage (1988) analyze the forces at the teeth of a drilling roller-cone bit (see part 2). They observe that higher torque values caused by vertical indentation and ROP correspond to weaker rocks. They observe also that part of the work expended to indent the vertical distance x_p is restituted in the form of elastic energy and results in a partial retraction of the rock, once the force of the retracting indenter has dropped to zero. They observe a rock retraction δ_x caused by an elastic restitution with a slope corresponding typically to a relative reduction of $\approx 1/5$ of x_p , i.e., (Figure 7) $\delta_x(x_p) \approx x_p/5$. Neglecting local permanent deformation effects, I have assumed that the indentation from 0 to x_p corresponds to the accumulation and restitution of elastic energy during the indentation process. I have also assumed that the force and elastic deformation are approximately in phase. The vertical force exerted by the bit tooth is assumed proportional to x_p . According to results of the complex-impedance analysis, the near-field phase of particle velocity can be expressed by a $\cos \tilde{\varphi}$ factor, where the symbol $\tilde{\varphi}$ means that the phase is averaged over

the range of frequencies of the signal. I assume that the amplitude of the vibration in phase with force is a fraction $\cos \tilde{\varphi}$ of the elastic restitution δ_x at the completion of the deformation and relaxation process, which is of magnitude $\delta_x = x_p/5$. The elastic-radiated power produced by the vertical action of the teeth can be estimated by substituting $(x_p^2/5) \cos \tilde{\varphi}$ in place of x_p^2 in the rotary-drilling equation 52. With these assumptions, the elastic power produced by the vertical force approximately equals $0.2 \cos \tilde{\varphi}$ times the vertical indentation power, in which a part of the rotary-drilling energy is transformed. This part is calculated from rotary-drilling equation 53 expressed in terms of drilling parameters, in which the ratio of the indentation power to the total power is $b_8 R_D^{1/n} / T_D$. Finally, the power of elastic vibration produced by the vertical force in the formation can be expressed in terms of the rotary equation as a fraction of the rotary power by

$$W_R \approx 0.2 \frac{b_8 R_D^{1/n}}{T_D} \frac{2\pi \times \text{TOB} \times \text{rpm}}{60} \cos \tilde{\varphi}, \quad (54)$$

or, by using only the dimensionless parameters,

$$\frac{W_R}{W_{\text{drill}}} \approx 0.2 \frac{b_8 R_D^{1/n}}{T_D} \cos \tilde{\varphi}, \quad (55)$$

where I have approximated the torque-rotary power as the total drilling power of equation 1. Equations 54 and 55 relate the average drilling conditions to local effects and the expenditure of elastic energy radiated from the bit assumed as a vertical source. The radiation model does not include transverse components, which are accounted for in the drilling equations. Moreover, the approach has the limitation that the experimental restitution value of $x_p/5$ is obtained while drilling rock specimens in the laboratory. The restitution occurring during full-scale drilling may be very different, and it is difficult to measure. Finally, the approach has the disadvantage that evaluation of the drilling-bit constant (b_8) may involve laborious analysis of drilling data sets and crossplots of drilling parameters with different bit types. Nevertheless, let us assume a milled roller-cone bit with $b_8 = 0.08$, $n = 2$ (as recommended by Sheppard and Lesage, 1988), ROP = 10 m/hour, TOB = 6 kNm, WOB = 98 kN, rpm = 120 rev/min, and $D = 12\frac{1}{4}$ in. We obtain from equations 55 and 38, for a 30-Hz source in a Poisson's formation of compressional velocity, $\alpha = 4200$ m/s ($\tan \tilde{\varphi} \approx 150$), $W_R / W_{\text{drill}} \approx 0.2 \times 0.0272 \times \cos \tilde{\varphi} \approx 0.36 \times 10^{-4}$. This value is in agreement — in order of magnitude — with the result E_R / E_0 calculated by Simon (1963).

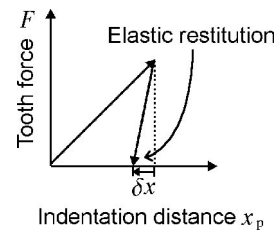


Figure 7. Penetration in rock, i.e., vertical indentation distance x_p and elastic restitution δ_x of displacement during a roller-cone tooth-indentation process (modified after Sheppard and Lesage, 1988).

PARTITION OF THE BOREHOLE AND RADIATED ENERGY

To analyze the partition of the radiated energy for SWD purposes, we have to consider also the energy transmitted in the drill string and in the borehole. Assume a vertical/axial force at the bit. In general, we have

$$W_{\text{vibr}} = W_{\text{R}} + W_1 + W_{\text{N}} + W_{\text{G}} + W_{\text{F}}, \quad (56)$$

where W_{R} is the power radiated by the vertical force in the formation in the far-field, W_1 is the power of the axial waves generated in the drill string by the reaction force, W_{N} is the power temporarily stored in the near-field and continuously exchanged with the drill string, W_{G} is the power radiated in the form of borehole- and mud-guided waves (Lea and Kyllingstad, 1996; Poletto et al., 2001), and W_{F} is flexural drill-string waves. I stress the following aspects:

- 1) The near-field term W_{N} has zero-mean value in time and does not contribute, on average, to the energy flux of the waves radiated in the formation and transmitted in the drill string.
- 2) The borehole interface and mud-guided waves, W_{G} , are important in borehole seismics, in particular with recording tools in the borehole (Lee and Balch, 1982). However, drill-bit seismic wavelengths are typically larger than the borehole radius, and we assume that the presence of the borehole does not substantially change the radiation pattern of the bit vertical force (Rector and Hardage, 1992). The axial force at the bit can produce a tangential stress acting in the axial direction at the borehole wall near the bit. White (1965, p. 226) shows that, with tangential stress, the “radiated displacements have the same form as displacements due to a point force.”
- 3) In our analysis, tube waves are not included in the source-radiation model. The conical-wave-radiated energy (Rector and Hardage, 1992; Heelan, 1953) is considered a product obtained at the expense of the drill-string propagating waves. As discussed before, this effect involves friction analysis. Previously, I estimated the bit vibrations induced by mud-pressure modulation; here, however, I do not calculate tube-wave contribution, W_{G} , in the energy balance of the bit source. The main reasons are the following: (1) We are interested in the partition of radiated-in-the-formation/drill-string pilot waves (say, near the bit) to determine the correlated energy; (2) SWD measurements are performed while rotary drilling. However, drilling necessarily involves mud circulation and hydraulic drilling. Drilling hydraulics has static and dynamic aspects (see, for instance, Maurer and Heilhecker, 1969), but it is not included in the mechanical rotary-energy model I use in equation 1. A study of the interactions between mud-pressure waves, bit forces, and drilling performance requires a separate analysis. The following hydraulic/acoustic aspects of drilling are important: properties of the mud circulation system, mud-flow regimes, Doppler effects, drill-string and bit geometry (in the cross sections exposed to mud pressure), bit-jet design, and downhole motor performance.

Hence, for simplicity in formulation of the energy balance of waves produced by a vertical force exerted on the drilled formation and on the drill string, I assume that $W_{\text{vibr}} \approx W_1 + W_{\text{R}}$. Assume, for simplicity, that the drill string is a tube with constant properties: cross section A_1 , density ρ_1 , and Young’s modulus Y_1 . The vertical reaction force at the bit, say $F = F_0 \sin \omega t$, produces stress axial-extensional vibrations that propagate in the drill string with rod velocity $c_1 = (Y_1/\rho_1)^{1/2}$ (Kolsky, 1953; Carcione and Poletto, 2000). Let z be the axial string coordinate and $\sigma_0 = -F_0/A_1$ the axial-stress magnitude at the bit ($z = 0$). In the absence of attenuation, the axial-stress wave induced in the drill string is

$$\sigma_1 = \sigma_0 \sin(\omega t - k_1 z), \quad (57)$$

where $k_1 = \omega/c_1$. The average elastic energy stored in the unit volume of the medium is given by (Jaeger, 1969)

$$E_1 = \frac{1}{2} \frac{\sigma_0^2}{Y_1}. \quad (58)$$

To obtain the average power of the stress wave propagating in the drill string, I multiply E_1 by the volume, $c_1 A_1$, traveled by the wave in the unit time, which gives

$$W_1 = \frac{1}{2} c_1 A_1 \frac{\sigma_0^2}{Y_1} = \frac{1}{2} \frac{F_0^2}{\mathcal{Z}_1}, \quad (59)$$

where I used $Y_1 = \rho_1 c_1^2$ and $\sigma_0 = F_0/A_1$, and where $\mathcal{Z}_1 = A_1 \rho_1 c_1$ is the characteristic (axial) impedance of the drill string (Lutz et al., 1972; Aarrestad et al., 1986) assumed as a rod. Note that, unlike for body waves radiated in the formation by the single-force harmonic source, the power transmitted by one-dimensional stress waves in homogeneous drill pipes does not depend on frequency. However, because the composition of the actual drill string is made up of sections of different acoustic impedances, the frequency response, i.e., the transfer function, of actual drill strings is not flat. Variation of impedances, signal reflectivity, energy transmission, and attenuation in actual drill strings are analyzed by Poletto et al. (2001) and Paslay and Bogy (1963).

Using equations 23 and 59, the ratio of drill-string to radiated-in-the-formation power can be expressed as

$$\frac{W_{\text{R}}}{W_1} = \frac{\mathcal{Z}_1}{\mathcal{Z}_{\text{R}}}. \quad (60)$$

For example, assume a 30-Hz wave radiated in a Poisson’s medium of P velocity $\alpha = 3160$ m/s and density $\rho = 2400$ kg/m³ when drilling with a drill collar of outer and inner diameters of 8.5 in. and 2.75 in., respectively; a bar velocity of 5130 m/s; and density of 7840 kg/m³. The obtained ratio of at-the-bit and radiated impedances is $\mathcal{Z}_1/\mathcal{Z}_{\text{R}}^{(P)} = 1.8 \times 10^{-4}$. In other words, we obtain $W_{\text{vibr}} \sim W_1$. This means that expenditure of the energy in the drill string can be more relevant for drilling-energy balancing than the energy radiated in the formation. The cross section of the drill collars is typically used for estimating the drill-string impedance \mathcal{Z}_1 at the bit (Poletto et al., 2000). Note that from equation 60, it follows that, by using thinner pipe sections, the amount of energy W_1 generated into the drill string increases, because the impedance $\mathcal{Z}_1 \propto A_1$ decreases.

Measuring power in the drill string

Assuming a monochromatic drill-string wave, we can calculate impedance and use force to measure the power of axial waves produced in the drill string and radiated in the formation. However, acceleration measurements are often available and can be used in place of force (Table 3). Peak-to-peak values of axial acceleration may range between a few *gs* under common drilling conditions (Cunningham, 1968; Deily et al. 1968; Eronini et al., 1982) and to tens of *gs* with anomalous drill-string pendulum vibrations of high amplitude (Dykstra et al., 1996). The average power of a monochromatic acceleration wave propagating in a uniform drill string is (see Appendix C)

$$W_1 = \frac{1}{2} Z_1 \frac{a_0^2}{\omega^2}, \quad (61)$$

where a_0 is the acceleration amplitude. However, in general, stationary waves are also generated in a drill string in contact with the formation at the bit.

Complex bit/rock reflection coefficient

The interaction between drill string and formation subject to vertical force is obtained by the axial-reflection coefficient at the bit. This coefficient can be calculated by using the drill-string impedance $Z_1 = A_1 \rho_1 c_1$ and the integrated complex impedance Z_b (equations B-7 or B-5) to calculate the reflection coefficient (Appendix D):

$$c_0 = \frac{Z_b - Z_1}{Z_b + Z_1}. \quad (62)$$

The coefficient c_0 can be used to calculate the frequency-dependent partition of stationary and upgoing waves in the drill string. Moreover, it can be related to the drilling conditions by using $Z_1 = A_1 \rho_1 c_1$ and equation D-11. We can inter-

Table 3. Axial force and acceleration magnitude in drill strings.

String component	Section (cm ²)	Harmonic frequency (Hz)	Force (kN)	Acceleration (g)
8-in. drill collar	286.0	6	100	0.33
8-in. drill collar	286.0	30	50	0.84
8-in. drill collar	286.0	80	10	0.44
5-in. heavy-weight drill pipe	81.1	6	100	1.18
5-in. heavy-weight drill pipe	81.1	30	50	2.95
5-in. heavy-weight drill pipe	81.1	80	10	1.57
5-in. drill pipe	34.1	6	100	2.80
5-in. drill pipe	34.1	30	50	7.01
5-in. drill pipe	34.1	80	10	3.74

pret the results in the following way: In the drill string, there is a traveling wave, which is usually assumed in SWD. However, there are also stationary waves sensitive to near-field vibrations of the rock. The partition is related to the phase angle $\varphi = \varphi(\alpha, \beta, r_b, \omega)$. This explains why, for instance, the detection of frequency resonances in relation to drilled-rock properties can be used for while-drilling acoustic-logging purposes (Lutz et al., 1972).

CONCLUSIONS

The energy expended during rotary drilling is analyzed for drill-bit SWD purposes. The theoretical calculation is aimed at quantifying the energy requirements, radiation properties, and near-field effects by relating drilling parameters to vibrations in the formation and in the drill string. Results show that a small part of the total drilling energy is transformed ultimately into radiated waves. The radiated power is quantified by assuming a single vertical force at the bit. The numerical results are used in part 2 of this paper to compare performances of the working drill bit and conventional borehole supporting sources.

ACKNOWLEDGMENTS

The author thanks Klaus Helbig for his invaluable suggestions and comments about near-field vibrations, Anthony Gangi for critical reading and many important comments to the work here presented, and Giorgia Pinna for her help in the bibliographic research. The author also thanks ENI-AGIP for supporting the research.

APPENDIX A

COEFFICIENTS OF HARMONIC NEAR-FIELD WAVES

Coefficients of radial (R) and shear-transverse (S) components

We use $f(t) = \sin \omega t$ in equation 30 and obtain equation 31 where

$$\begin{aligned} R_0 &= \frac{F_0 \cos \phi}{4\pi \rho r \alpha^2}, & S_0 &= \frac{F_0 \sin \phi}{4\pi \rho r \beta^2} \\ R_1 &= 1 - \frac{2\alpha^2}{r^2 \omega^2}, & S_1 &= -1 + \frac{\beta^2}{r^2 \omega^2}, \\ R_2 &= -\frac{2\alpha}{r\omega}, & S_2 &= \frac{\beta}{r\omega}, \\ R_3 &= \frac{2\alpha^2}{\beta r \omega}, & S_3 &= -\frac{\beta^2}{\alpha r \omega}, \\ R_4 &= \frac{2\alpha^2}{r^2 \omega^2}, & S_4 &= -\frac{\beta^2}{r^2 \omega^2}. \end{aligned} \quad (A-1)$$

Coefficients of harmonic sine and cosine components

For the radial displacement component, we have the coefficients

$$\begin{aligned} Q_1 &= R_1 \cos k_\alpha r + R_2 \sin k_\alpha r + R_3 \sin k_\beta r + R_4 \cos k_\beta r, \\ Q_2 &= -R_1 \sin k_\alpha r + R_2 \cos k_\alpha r + R_3 \cos k_\beta r - R_4 \sin k_\beta r, \end{aligned} \quad (A-2)$$

where $k_\alpha = \omega/\alpha$ and $k_\beta = \omega/\beta$. Similar relations are obtained for the transverse-displacement component by substituting S_i in place of R_i and interchanging k_α and k_β , which gives

$$\begin{aligned} Q_3 &= S_1 \cos k_\beta r + S_2 \sin k_\beta r + S_3 \sin k_\alpha r + S_4 \cos k_\alpha r, \\ Q_4 &= -S_1 \sin k_\beta r + S_2 \cos k_\beta r + S_3 \cos k_\alpha r - S_4 \sin k_\alpha r. \end{aligned} \quad (\text{A-3})$$

Near-field approximation of Q_i (lim $k_\alpha r \rightarrow 0$)

We have

$$\begin{aligned} Q_1 &\rightarrow 3, \\ Q_2 &\rightarrow -k_\alpha r \left(\frac{1}{3} + 2\sqrt{3} \right), \\ Q_3 &\rightarrow -\frac{2}{3}, \\ Q_4 &\rightarrow k_\alpha r (1 + 6\sqrt{3})/9. \end{aligned} \quad (\text{A-4})$$

APPENDIX B COMPLEX IMPEDANCE

It is convenient to rewrite particle velocity and stress in a complex form. We can use the near-field approximation of equation 40 to write the axial particle velocity at the bit (see equation 43) as the complex velocity

$$v_0 = \iota V_0 e^{\iota(\omega t - \varphi)}, \quad (\text{B-1})$$

where

$$V_0 = \frac{F_0 k_\alpha r_b}{A_b \rho \alpha \sin \varphi}, \quad (\text{B-2})$$

so that the real part of equation B-1 equals the real velocity of equation 43. Moreover, the axial stress becomes

$$\sigma_0 = -\iota \frac{F_0}{A_b} e^{\iota \omega t}. \quad (\text{B-3})$$

The radiation impedance is therefore calculated as

$$\frac{\sigma_0}{v_0} = -\frac{F_0}{A_b V_0} e^{\iota \varphi} = -\frac{\rho \alpha}{k_\alpha r_b} (\cos \varphi \sin \varphi + \iota \sin^2 \varphi). \quad (\text{B-4})$$

The impedance of equation B-4 is calculated in the near-field approximation. The near-field integrated impedance over the bit area is

$$\mathcal{Z}_b = \frac{A_b \sigma_0}{v_0} = -\frac{A_b \rho \alpha}{k_\alpha r_b} (\cos \varphi \sin \varphi + \iota \sin^2 \varphi). \quad (\text{B-5})$$

Now we relate the near- and far-field integrated impedances. We observe that the total integrated impedance of equation 27 can be expressed as

$$\mathcal{Z}_R^{(P)} = -\frac{A_b \rho \alpha}{k_\alpha r_b} \tan \varphi. \quad (\text{B-6})$$

We obtain

$$\mathcal{Z}_b = \mathcal{Z}_R^{(P)} (\cos^2 \varphi + \iota \cos \varphi \sin \varphi). \quad (\text{B-7})$$

APPENDIX C

POWER OF AXIAL DRILL-STRING WAVES

Let the axial acceleration be expressed as

$$a_1 = a_0 e^{\iota(\omega t + k_1 z)}, \quad (\text{C-1})$$

$$a_1 = \frac{\partial^2 u_1}{\partial t^2} = -\omega^2 u_1, \quad (\text{C-2})$$

where u_1 is the axial displacement in the drill string. Values of peak-to-peak axial displacement ranging from about 0.5 to 2 in. were observed by Cunningham (1968). The axial displacement is related to the axial stress σ_1 by

$$\sigma_1 = Y_1 \frac{\partial u_1}{\partial z} = \iota Y_1 k_1 u_1. \quad (\text{C-3})$$

Using $k_1 = \omega/c_1$, $\sigma_1 = F/A_1$, and the characteristic impedance of drill-string axial waves $\mathcal{Z}_1 = A_1 \rho_1 c_1$, we obtain (see Table 3)

$$F = -\iota \frac{\mathcal{Z}_1 a_1}{\omega}. \quad (\text{C-4})$$

Taking the time-average value of $\Re[F]^2$, where \Re denotes the real part, hence of $\Re[a_1]^2$ over T from equation 59, we have

$$W_1 = \frac{\mathcal{Z}_1 a_0^2}{2\omega^2}. \quad (\text{C-5})$$

Using equation C-5, the drill-string power can be calculated from field MWD acceleration measurements in the drill pipes, which can be related to acceleration at the bit using the drill-string transfer function.

APPENDIX D

COMPLEX REFLECTION COEFFICIENT AT THE BIT

I calculated the near-field phase of sine and cosine waves in the formation in contact to the bit (assumed flat and in perfect contact to the rock) with a time-harmonic force at the bit. If the drill string (uniform and of infinite height above the bit) were isolated, the harmonic force would generate simple harmonic waves in the drill string itself. However, coupling to the formation subject to the near-field vibrations introduces both in-phase and out-of-phase components in the string. Let us assume that the harmonic axial stress is uniform over the pipe cross section A_1 and that it is given at the near-bit/rock interface depth ($z = 0$) as the real part of

$$\sigma_1(\omega, z = 0) = \iota \frac{F_0}{A_1} e^{\iota \omega t}. \quad (\text{D-1})$$

We assume that the complex axial stress in the drill string is

$$\sigma_1 = A \sigma_D + R \sigma_U = A e^{\iota(\omega t - k_1 z)} + R e^{\iota(\omega t + k_1 z)}, \quad (\text{D-2})$$

where σ_D is a downgoing time-harmonic stress-wave incident at the bit/rock interface from above, σ_U is the upgoing harmonic stress wave reflected at the interface, and A and R are complex coefficients. We assume continuity of stress at the bit/rock contact $z = 0$. From equations D-1 and D-2, we have

$$A + R = \iota \frac{F_0}{A_1}. \quad (\text{D-3})$$

Therefore, the relations for the real and imaginary parts are

$$\begin{aligned}\Re[R] &= -\Re[A], \\ \Im[R] &= -\Im[A] + \frac{F_0}{A_1}.\end{aligned}\quad (\text{D-4})$$

Using equation D-3 in equation D-2, we obtain

$$\sigma_1(\omega, z) = A\sigma_D - \left(A - i\frac{F_0}{A_1}\right)\sigma_U, \quad (\text{D-5})$$

from which we have

$$\sigma_1(\omega, z) = -2iA \sin(k_1 z) e^{i\omega t} + i\frac{F_0}{A_1} e^{i(\omega t + k_1 z)}. \quad (\text{D-6})$$

The first term on the right is a stationary wave of amplitude zero at the bit; the second term on the right is an upgoing stress wave of amplitude F_0/A_1 .

Complex bit/rock coefficient

To determine the complex reflection coefficient, I equal the axial displacements u_1 in the drill string near the bit and the axial displacement in the formation u_0 at the bit/rock contact ($z = 0$) (equation 35):

$$u_1 = u_0 = \lim_{h \rightarrow 0} \hat{u}. \quad (\text{D-7})$$

In the drill string, we have $\sigma_1 = Y_1 \partial u_1 / \partial z$, and from $Y_1 k_1 = \omega \rho_1 c_1$, we obtain

$$u_1 = A \frac{\sigma_D}{-i\omega \rho_1 c_1} + R \frac{\sigma_U}{i\omega \rho_1 c_1}, \quad (\text{D-8})$$

and from equation D-3, we obtain

$$u_1 = i \frac{A}{\omega \rho_1 c_1} (\sigma_D + \sigma_U) + \frac{F_0 \sigma_U}{\omega A_1 \rho_1 c_1}. \quad (\text{D-9})$$

From equation B-1 and from $v_0 = i\omega u_0$, we have in the formation

$$u_0 = -\frac{F_0 r_b}{A_b \rho \alpha^2} (t - \cot \varphi) e^{i\omega t}, \quad (\text{D-10})$$

with the phase (given from equation 40)

$$\cot \varphi = -\frac{k_\alpha r_b (1 + 6\sqrt{3})}{12}. \quad (\text{D-11})$$

Using equation D-1, we obtain

$$\begin{aligned}A &= \frac{F_0}{2i A_1} \frac{1}{A_b \rho \alpha} [-k_\alpha r_b (t - \cot \varphi) A_1 \rho_1 c_1 - A_b \rho \alpha], \\ R &= \frac{F_0}{2i A_1} \frac{1}{A_b \rho \alpha} [k_\alpha r_b (t - \cot \varphi) A_1 \rho_1 c_1 - A_b \rho \alpha].\end{aligned}\quad (\text{D-12})$$

The complex bit/rock reflection coefficient is obtained as

$$c_0 = \frac{R}{A}. \quad (\text{D-13})$$

which, after calculations based on previous equations, becomes

$$c_0 = \frac{A_\alpha \rho \alpha (k_\alpha r_b)^{-1} (\cos \varphi \sin \varphi + i \sin^2 \varphi) + A_1 \rho_1 c_1}{A_\alpha \rho \alpha (k_\alpha r_b)^{-1} (\cos \varphi \sin \varphi + i \sin^2 \varphi) - A_1 \rho_1 c_1}. \quad (\text{D-14})$$

We obtain an equivalent result if we use the drill-string impedance $Z_1 = A_1 \rho_1 c_1$ and the integrated complex impedance Z_b of equation B-5 to calculate the coefficient

$$c_0 = \frac{Z_b - Z_1}{Z_b + Z_1}. \quad (\text{D-15})$$

REFERENCES

- Aarrestad, T. V., H. A. Tønnesen, and A. Kyllingstad, 1986, Drill-string vibrations: Comparison between theory and experiments on a full-scale research drilling rig: IADC/SPE Paper No. 14760.
- Aki, K., and P. G. Richards, 1980, Quantitative seismology — Theory and methods, Vol. I: W. H. Freeman and Company.
- Baeten, G., and A. Ziolkowski, 1990, The vibroseis source: Elsevier Science Publishing Co.
- Bernabe, Y., and W. F. Brace, 1990, Deformation and fracture of Berea sandstone: The brittle/ductile transition in rocks: American Geophysical Union, Geophysical Monographs, **56**, 91–101.
- Biggs, M. D., J. B. Cheatham Jr., and U. Rice, 1969, Theoretical forces for prescribed motion of a roller bit: SPE Paper No. 2391.
- Bourgoyne Jr., A. T., K. K. Millheim, M. E. Chenevert, and F. S. Young Jr., 1991, Applied drilling engineering, Vol. 2: SPE Textbook Series.
- Burgess, T. M., and W. G. Lesso Jr. 1985, Measuring the wear of milled tooth bits using MWD torque and weight-on-bit: SPE/IADC Paper No. 13475.
- Carcione, J. M., and P. M. Carrion, 1992, 3-D radiation pattern of the drilling bit source in finely stratified media: Geophysical Research Letters, **19**, no. 7, 717–720.
- Carcione, J. M., and F. Poletto, 2000, Simulation of stress waves in attenuating drill strings, including piezoelectric sources and sensors: Journal of the Acoustic Society of America, **108**, no. 1, 53–64.
- Cassand, J., and M. Lavergne, 1971, Seismic emission by vibrators: Seismic filtering: SEG, Translation of Editions Technip, 198.
- Clayer, F., J. K. Vandiver, and H. Y. Lee, 1990, The effect of surface and downhole boundary conditions on the vibration of drillstrings: SPE Paper No. 20447.
- Cunningham, R. A., 1968, Analysis of downhole measurements of drill string forces and motions: Journal of Engineering for Industry, Transactions of the ASME, Series B, **90**, 209–216.
- Deily, F. H., D. W. Dareing, G. H. Paff, J. E. Orloff, and R. D. Lynn, 1968, Downhole measurements of drill string forces and motions: Journal of Engineering for Industry, Transactions of the ASME, Series B, **90**, 217–225.
- Devereux, S., 1998, Practical well planning and drilling manual: PennWell Publishing Co.
- , 1999, Drilling technology in nontechnical language: PennWell Publishing Co.
- Dykstra, M. W., D. C.-K. Chen, T. M. Warren, and J. J. Azar, 1996, Drillstring component mass imbalance: A major source of downhole vibrations: SPE Drilling & Completion, SPE Paper No. 29350-P, December, 234–241.
- Eronimi, I. E., W. H. Somerton, and D. M. Auslander, 1982, A dynamic model for rotary rock drilling: ASME Journal of Energy Resources Technology, **104**, 108–120.
- Falconer, I. G., T. M. Burgess, and M. C. Sheppard, 1988, Separating bit and lithology effects from drilling mechanics data: IADC/SPE Paper No. 17191.
- Falconer, I. G., J. P. Belaskie, and F. Varlava, 1989, Application of a real time wellbore friction analysis: SPE Paper No. 18649.
- Gabolde, G., and J. P. Nguyen, 1999, Drilling data handbook, 7th ed.: Editions Technip.
- Gangi, A. F., 1987, A theoretical study of the radiation patterns of a tunnel-boring machine (infinite medium): Texas A&M University, Final Report GL-87-20.
- Haldorsen, J. B. U., D. E. Miller, and J. J. Walsh, 1995, Walk-away VSP using drill noise as a source: Geophysics, **60**, 978–997.
- Hardage, B. A., 1992, Crosswell seismology and reverse VSP: Geophysical Press.
- Heelan, P. A., 1953, Radiation from a cylindrical source of finite length: Geophysics, **18**, 685–696.
- Hokstad, K., R. Sollie, and I. M. Charlsen, 2001, VSP while drilling for geosteering applications: 71st Annual International Meeting, SEG, Expanded Abstracts, 452–455.
- Hunter, S. C., 1957, Energy absorbed by elastic waves during impact: Journal of the Mechanics and Physics of Solids, **5**, 162–171.
- Jaeger, J. C., 1969, Elasticity, fracture and flow with engineering and geological applications: Science Paperbacks **55**.

- Kaufman, A. A., and A. L. Levshin, 2000, Acoustic and elastic wave fields in geophysics, I; Elsevier Science Publishing Co.
- Kolsky, H., 1953, Stress waves in solids: Oxford University Press.
- Langeveld, C. J., 1992, PDC Bit Dynamics: IADC/SPE Paper No. 23867.
- Lea, L. H., and Å. Kyllingstad, 1996, Propagation of coupled pressure waves in borehole with drillstring: SPE Paper No. 37156.
- Lee, M. W., and A. H. Balch, 1982, Theoretical seismic wave radiation from a fluid-filled borehole: *Geophysics*, **47**, 1308–1314.
- Lesage, M., I. G. Falconer, and C. J. Wick, 1988, Evaluation drilling practice in deviated wells with torque and weight data: SPE Drilling Engineering, September, SPE Paper No. 16114, 248–252.
- Lesso, W. G., and S. V. Kashikar, 1996, The principles and procedures of geosteering: IADC/SPE Paper No. 35051.
- Love, A. E. H., 1944, A treatise on the mathematical theory of elasticity, 4th ed.: Cambridge University Press.
- Lutz, J., M. Raynaud, S. Gastalder, C. Quichaud, J. Raynald, and J. A. Muckerloy, 1972, Instantaneous logging based on a dynamic theory of drilling: *Journal of Petroleum Technology*, June, 750–758.
- Ma, D., D. Zhou, and R. Deng, 1995, The computer simulation of the interaction between roller bit and rocks: SPE Paper No. 29922.
- Maurer, W. C., 1965, Shear failure of rock under compression: SPE Paper No. 1054.
- Maurer, W. C., and J. K. Heilhecker, 1969, Hydraulic jet drilling: SPE Paper No. 2434.
- Miller, G. F., and H. Pursey, 1954, The field and radiation impedance of mechanical radiators on the free surface of semi-infinite isotropic solid: *Proceeding of the Royal Society*, **223**, 521–541.
- Miranda, F., L. Aleotti, F. Abramo, F. Poletto, A. Craglietto, S. Persoglia, and F. Rocca, 1996, Impact of seismic while drilling technique on exploration wells: *First Break*, **14**, 55–68.
- Moore, P. L., 1986, Drilling practices manual, 2nd ed.: PennWell Publishing Co.
- Olgaard, D. L., and W. F. Brace, 1983, The microstructure of gouge from a mining-induced seismic shear zone: *International Journal of Rock Mechanics and Geomechanical Abstracts*, **20**, 11–19.
- Paslay, P. R., and D. B. Bogy, 1963, Drill string vibrations due to intermittent contact of bit teeth: *Journal of Engineering for Industry*, Transactions of ASME, 187–194.
- Pessier, R. C., and M. J. Fear, 1992, Quantifying common drilling problems with mechanical-specific energy and a bit-specific coefficient of sliding friction: SPE Paper No. 24584.
- Pilant, W., 1979, Elastic waves in the Earth: Elsevier Science Publishing Co.
- Poletto, F., 2005, Energy balance of a drill-bit seismic source, part 2: Drill bit versus conventional seismic sources: *Geophysics*, this issue.
- Poletto, F., and F. Miranda, 1998, Seismic while drilling use of pilot signals with downhole motor drilling: SEG 68th Annual International Meeting, Extended Abstracts, ACQ-4.5.
- Poletto, F., F. Miranda, P. Corubolo, and F. Abramo, 1997, Seismic while drilling using PDC signals — Seisbit experience and perspectives: 59th Annual International Meeting, EAGE, Extended Abstracts, E-053.
- Poletto, F., F. Rocca, and L. Bertelli, 2000, Drill-bit signal separation for RVSP using statistical independence: *Geophysics*, **65**, 1654–1659.
- Poletto, F., M. Malusa, and F. Miranda, 2001, Numerical modeling and interpretation of drill-string waves: *Geophysics*, **66**, 1569–1581.
- Rabia, H., 1985, Specific energy as a criterion for bit selection: *Journal of Petroleum Technology*, July, SPE Paper No. 12355, 1225–1229.
- Rector III, J. W., and B. P. Marion, 1991, The use of drill-bit energy as a downhole seismic source: *Geophysics*, **56**, 628–634.
- Rector III, J. W., and B. A. Hardage, 1992, Radiation pattern and seismic waves generated by a working roller-cone drill bit: *Geophysics*, **57**, 1319–1333.
- Sheppard, M. C., and M. Lesage, 1988, The forces at the teeth of a drilling rollercone bit: Theory and experiment: SPE Paper No. 18042.
- Simon, R., 1963, Energy balance in rock drilling: *Society of Petroleum Engineers Journal*, December, SPE Paper No. 499, 298–306.
- Somerton, W. H., A. Timur, and D. H. Gray, 1961, Stress behavior of rock under drilling loading conditions: SPE Paper No. 166.
- Staron, P., G. Arens, and P. Gros, 1988, Method of instantaneous acoustic logging within a wellbore: U.S. patent 4 718 048.
- White, J. E., 1965, Seismic waves: Radiation, transmission, and attenuation: McGraw-Hill Book Co.